

International Journal of Emerging Electric Power Systems

Volume 10, Issue 1

2009

Article 1

Magnetizing Switching Inrush: Estimation and a Novel Circuitry for Inrush Elimination

Sharmili Das, *Indian Institute of Technology, Kharagpur*

Dinkar Prasad, *Emerson Network Power India Ltd*

Tapas Kumar Bhattacharya, *Indian Institute of
Technology, Kharagpur*

S. SenGupta, *Indian Institute of Technology, Kharagpur*

Recommended Citation:

Das, Sharmili; Prasad, Dinkar; Bhattacharya, Tapas Kumar; and SenGupta, S. (2009)
"Magnetizing Switching Inrush: Estimation and a Novel Circuitry for Inrush Elimination,"
International Journal of Emerging Electric Power Systems: Vol. 10: Iss. 1, Article 1.
DOI: 10.2202/1553-779X.1870

Magnetizing Switching Inrush: Estimation and a Novel Circuitry for Inrush Elimination

Sharmili Das, Dinkar Prasad, Tapas Kumar Bhattacharya, and S. SenGupta

Abstract

A power transformer, when energized at no-load, may have transient currents up to 100 times that of the steady state magnetizing current. This inrush current has several detrimental effects on power quality and may damage sensitive equipment connected to the system. In this paper, a power electronic based control circuit is developed, which estimates the last remnant and, utilizing this data, it controls the next re-energization instant to achieve inrush free switching. An equivalent circuit model of a transformer is also presented to simulate the transient dynamic performance of a transformer for any arbitrary switching operation.

KEYWORDS: residual flux, inrush currents, controlled switching, prospective flux, point on wave switching

Author Notes: Dr. S. Das is from the Department Electrical Engineering, National Institute of Technology, Rourkela-769008. T.K. Bhattacharya and S. SenGupta are professors from the Department of Electrical Engineering, Indian Institute of Technology, Kharagpur-721303. Dr. Dinkar Prasad is with the Emerson Network Power (India) Ltd.

I. INTRODUCTION

Typical magnetization characteristics of the transformer core exhibit considerable non-linearity beyond the knee point. The non-linearity is due to hysteresis and saturation behaviors of ferromagnetic core. Random energization of the transformer may drive the core flux to grow deeper into the saturation zone. During this operation, transformer draws a huge current (400 times the steady state magnetizing current) for initial few cycles. Several numerical and analytical models (Ling and Basak (1988), Ogawa (2002), Len et al.(1993), Khalifah and Saadany (2006)) have been proposed to analyze the phenomenon. This phenomenon is termed as magnetizing switching inrush and it is well reported in the literature. This high current rich in harmonics, has many adverse effects such as nuisance tripping of circuit breaker, confusion in over current relay (Kasztenny (2006)) operation, mechanical damage to the transformer windings (Steurer and Frohlich (2002)), deterioration of insulation, voltage drop (Cui et al.(2005), Xu et al.(2005)) etc. Due to these undesirable effects, inrush currents have always been a concern in power industry. Over the past few decades, a few methods have been put forwarded to suppress the inrush currents. These includes modifying the core design (Cheng et al.(2004)), insertion of resistance in neutral line with sequential phase energization (Cui et al.(2005), Xu et al.(2005), Abdulsalam and Xu (2007)) soft starting, series compensator (Shyu (2005)) and controlled switching scheme (Brunke and Frohlich (2001a), Brunke and Frohlich (2001b), Asghar (1996)). Incorporation of auxiliary winding or re-designing the core as suggested in scheme (Cheng et al.(2004)) increases manufacturing costs.

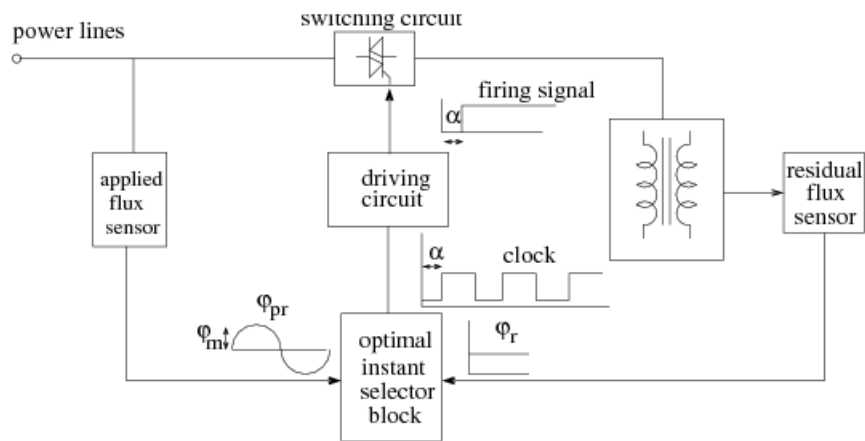


Fig.1. Basic Control Logic for Inrush minimization scheme.

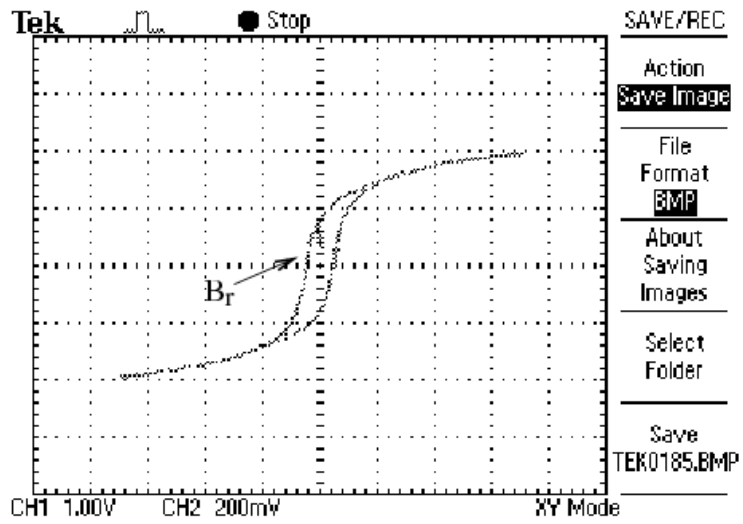
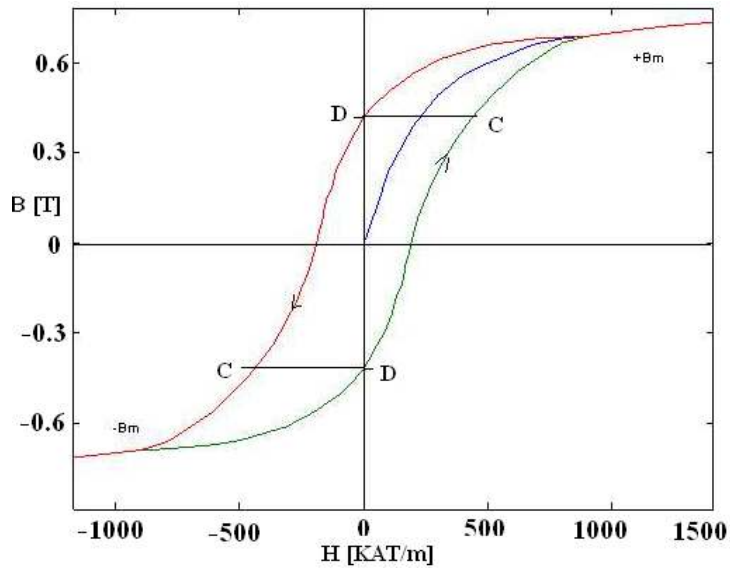
By inserting resistance along with neutral line will cause power loss as well as further voltage dip. Soft starting with reduced initial applied voltage switching-ON may not be practically attractive for critical loads. In series compensation, method another transformer in series with the main transformer is used, so its transient effects decrease the system efficiency increasing the cost.

It is well known that, the nature and extent of inrush depends primarily upon: (i). the point of energization on supply voltage wave, (ii). the magnitude and polarity of the residual flux left in the core prior to re-energization. Other factors like stray capacitance of the transformer and the connected transmission line, time lag of the circuit breaker opening and closing operation also affects the inrush. All these factors contribute to flux level mismatching between the earlier retained core flux (i.e., residual) and the applied flux at the energization point, which leads to inrush. Considering these facts, here a novel analog controller circuit is proposed and implemented, which controls the switching instants as such to minimize the core flux over-fluxing and subsequent saturation.

The developed controller circuit (shown in Fig.1), on line detects the de-energization instants and simultaneously tracks and records the residual flux level. Utilizing this remnant information, the controller selects the next favorable switching instant and triggers the solid-state switch to re-energize the transformer optimally. A theoretical model of transformer is also presented. This model describes the interdependency between electrical and magnetic variables and can predict the operating performance of the test transformer under both steady and transient operation. Both the theoretical and experimental results obtained are in close agreement.

II. PROPOSED APPROACH FOR INRUSH MITIGATION

At the time of energization, it is likely that the core is having some residual flux. Naturally, arbitrary switching-ON will cause the flux to build up from this remnant level and may drive the core into deeper saturation, causing heavy inrush current. The offset due to mismatch between the residual and prospective or applied flux dies down after few cycles, then the core flux and current settles within its steady-state limits. Therefore, the basis to limit inrush is by nullifying the effect of flux asymmetry due to core over fluxing. The technique implemented in the proposed scheme is to control the power-ON instant voltage levels, so that the flux linkage of transformer does not exceed the steady-state limit. Here next switching-ON is carried out in such a manner that the applied flux (i.e., prospective flux) matches last remnant resulting in practically zero dc offset or no flux asymmetry during initial core-flux characteristics. Core flux builds up from the remnant level in a steady state sinusoidal manner minimizing switching transients.



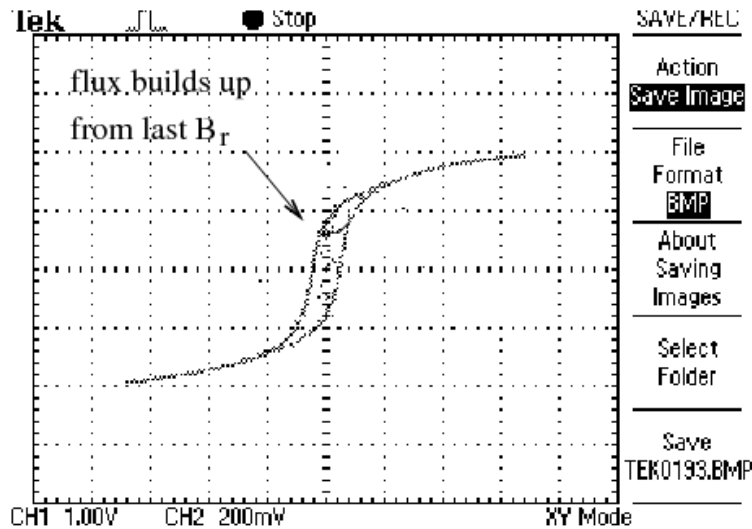


Fig.2. Typical magnetization characteristics of transformer, showing a specific remnant B_r level corresponds to two H values, Switching off instant B-H loop storing the B_r (remnant) and the next switching-on instant B-H loop starting from last B_r value. CH1 records H value; 1V=500 AT/m and CH2 records B_m value; 200 mV=0.4 T.

A particular remnant level (B_r) corresponds to two different points on the prospective flux wave pattern. If these two points are mapped onto the B-H curve (shown in Fig.2), then they correspond to two different values (C, D) of H or magnetizing current i_m . Zero flux error and minimum current error at switch-on may be obtained if of these two points (C and D), the one corresponding to minimum H , i.e., D is selected.

Experiments have been performed for a specific de-energization instant and the corresponding residual flux levels are stored in Fig.2. At the next turn on, the transformer is re-energized with a flux equal to the last remnant value. Substantial reduction of switching transients was realized. The same process have also been simulated referring theoretical approach and shown in Fig.17. The simulated and experimental results, so obtained, exhibit excellent correspondence. Two switches, one electro-mechanical (i.e., circuit breaker SW1 and a solid-state switch (triac) SW2) are connected in series with the transformer primary for de-energization and energization purpose respectively. Both the switches have their auxiliary control circuitry to control the energization and de-energization instants. The secondary may be kept open or connected to a load. The same controller works independent of the transformer rating.

III. DESCRIPTION OF SYSTEM HARDWARE

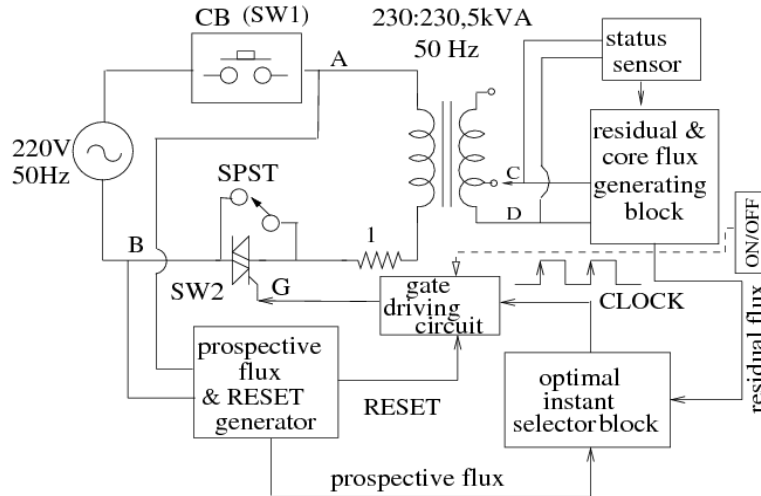


Fig.3. Block diagram of the proposed controller circuit along with the test transformer.

A. System Description

Controller block is isolated from the power circuit by a step down transformer. The transformer (230/230V, 5kVA) is powered from the ac mains only when both the switches are made ON. Similarly, transformer is de-energized by opening any one of them. The controller senses and tracks the secondary winding voltage and the input supply voltage to derive respective core flux and applied flux signals. The controller also senses the power-interruption point. Then with both the residual and applied flux information, the optimal instant selector block decides the next suitable energization instant. At the selected instants, the gate drive circuit sends triggering command to triac. This in turn re-energizes the transformer. The scaling of the sensed flux and the prospective flux are chosen in such a way that matching of levels and phase be ensured at each instant in steady state. Fig.4 shows typical results of one inrush-free re-energization instant by implementing the controller. Here arbitrary interruption of transformer is initiated at $\alpha = 128^\circ$, whereas actual turn-off occurs $\alpha = 68.3^\circ$. During de-energization residual settles to -0.37 pu. Then at next re-energization controller automatically fires the gate pulse of triac switch at $\alpha = 68.4^\circ$ to achieve inrush-free operation.

1. *Residual flux sensing block:* This unit (shown in Fig.5) comprises of a scale changer, integrator, status sensing circuit, ADC, DAC, 555 multi-vibrators. Voltage level between 86.6 % and 100 % tap position of the secondary terminal is taken as the input to the residual block. This input voltage level is then transformed into corresponding core flux signal by an integrator circuit. The

integrator is designed to capture transient signals upto 0.1MHz frequency range during switching-OFF operation. The integrator output (i.e., core flux) goes to the ADC to enable the storing of the value in digital form. The conversion and storage process continues as long as the clock and supply to ADC are ON. Once the transformer is de-energized, the status sensor circuit senses the transition point. This in turn changes the state of RESET pin of 555 MV from HIGH to LOW and it stops generating clock pulses thereafter. Now, ADC also stops further conversion process and latch on to the last converted value of core flux at supply interruption point (i.e., the remnant level). A hybrid ADC-DAC combination is used to retrieve back the original core flux signal in analog form. An intermediate digital storage is used to avoid the leakage component, which decays the analog value with time.

The transformer status sensing block has the same input as that of the residual block. The input voltage is rectified and compared with a very small dc voltage level. Therefore, as long as ac supply to transformer is maintained, output of the comparator is HIGH. This indicates the ON state of the transformer. When the supply to transformer is interrupted, then the comparator output changes its state from HIGH to LOW. HIGH and LOW states of the RESET pin corresponds to the ON/OFF status of the transformer and the transition edge corresponds to the switching instants. Whenever the supply to transformer is interrupted, the clock pulses are disabled and the core flux settles to a new dc remnant level. In this block 555 MV is capable of generating a clock pulse of 200 KHz, so that ADC can sample and track any high frequency transients. Integrator is also designed to compatible with the same. Representative residual flux patterns corresponding to switching-off instant $\alpha = 128^\circ$ is shown in Fig.4. Residual flux ϕ_r settles to -0.37 pu.

2. Prospective flux and RESET generating unit: This unit estimates the levels of steady state flux corresponding to different energization point. It consists of a scale changer, integrator, voltage sensor, delay circuit, comparator (shown in Fig.6). A replica of exact core flux (prospective flux) is generated whenever the supply is available after the CB is made ON.

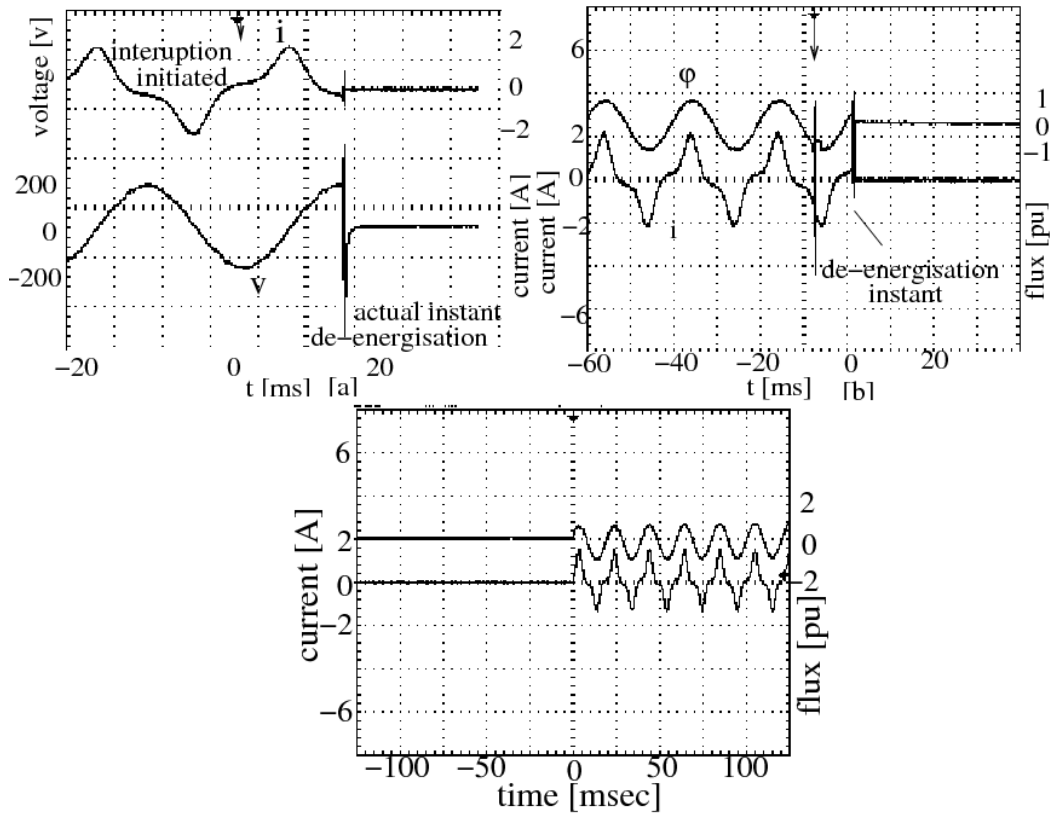


Fig.4. Test waveforms (voltage, current, flux) of arbitrary switching off instants, Test waveforms (flux, current) of controlled inrush-free re-energization instants.

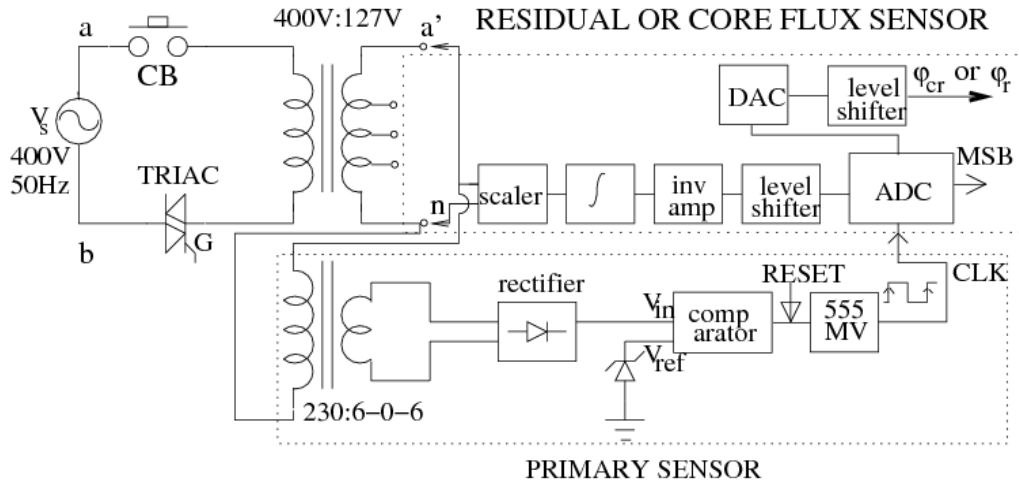


Fig.5. Block diagram of residual flux sensing unit.

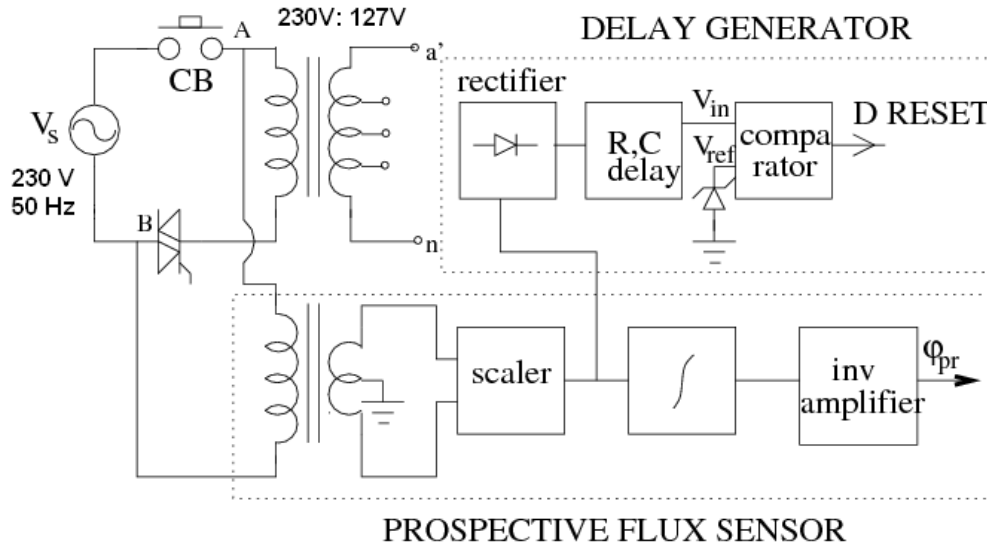


Fig.6. Block diagram of Prospective-flux, delay-generating unit.

The voltage at CB output (point A fig.6) is tapped and then this voltage level is integrated to derive a signal representing the prospective flux. Parameters of the integrator are properly chosen that estimated core flux and prospective flux is replica of each other during steady operation. Immediately after the CB is made ON, the integrator output may not represent the actual applied flux levels due to the transient behavior of sensing circuit and the control transformer. Hence during this interval if this erroneous applied flux signal is fed to optimal instant selector block, it will select an erroneous re-energization instant. To block this erroneous triggering of TRIAC (shown in Fig.3), an adjustable delay circuit is included after the integrator. This circuit blocks initial few cycles of the prospective flux until it reaches final steady-state limits. Within this delay interval, RESET pin of D-FF (which generates gate pulse for TRIAC) is maintained HIGH, so that gate drive signal of TRIAC is inhibited.

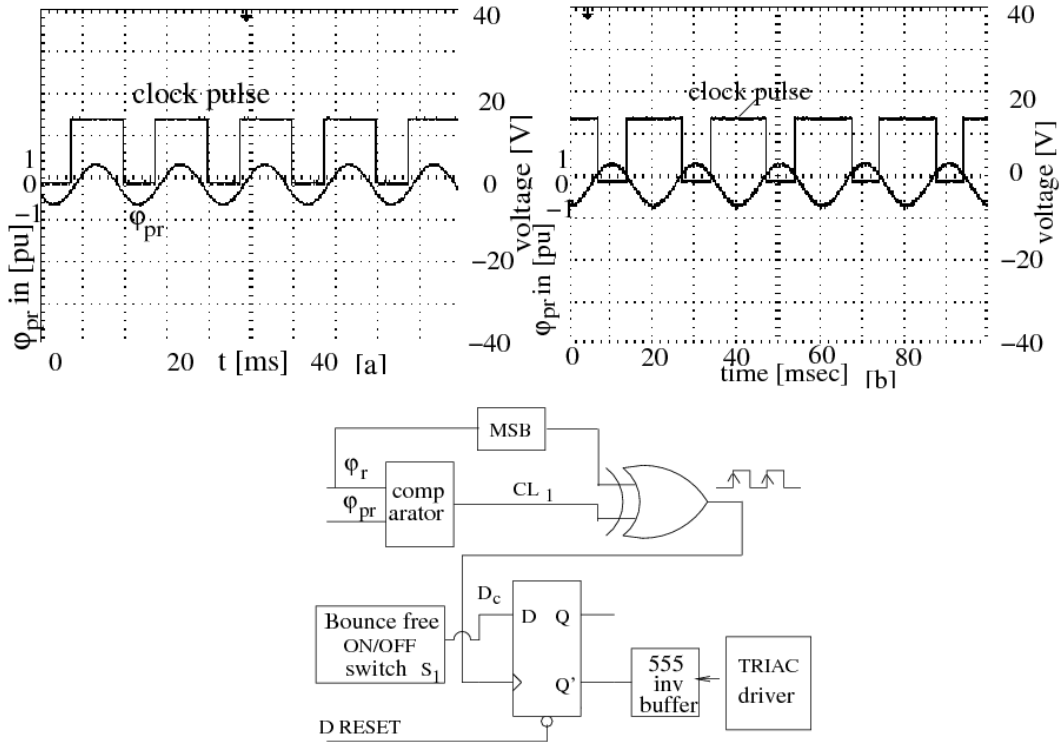


Fig.7. Block diagram of optimal switching instant selector block; Optimal clock pulse test waveforms obtained for different residual flux levels; [a] $\phi_r = -0.37$ pu and [b] $\phi_r = 0.214$ pu respectively (Experimental results).

3. *Optimum switching instant selection block*: The main component of this block (fig.7) are comparator, EX-OR logic gate, bounce-free ON/OFF switch, D-FF and a 555 inverting buffer. The bounce-free switch (S_1) generates the switching command (i.e., D_c) for transformer operation. HIGH and LOW of D_c corresponds to ON and OFF command respectively. The inputs to this block are the two flux levels, polarity of remnant and the RESET input of D-FF. The comparator compares the flux signals and generates rectangular pulses. The transition edge of the pulses corresponds to the instants when the flux levels (i.e., ϕ_{pr} and ϕ_r) are matched. The polarity of the remnant is obtained by tapping the MSB output of ADC. The MSB signal along with the comparator output is fed to the EX-OR gate to generate the desired clock pulses for the D-FF. The rising edge of the pulse corresponds to the optimum switch-ON instant of the transformer, where both the flux levels are matched and there is minimum current error (corresponding to point “D” of fig.2). The switching command is then transferred to the gate driving circuit to trigger the triac at the rising edge of the next clock pulse, following the transition from HIGH to LOW of the RESET

signal. In this way optimal re-energization of transformer is carried out. IC 555 provides the necessary current amplification to the driver circuit. Fig.7 shows the test results of desired gate pulses for two different de-energization instants with residual flux levels $\phi_r = -0.37$ pu [a] and 0.24 pu value [b] respectively.

4. *Arbitrary de-energization or current chopping*: To study the efficacy of the proposed scheme under various residual flux levels, it is required to obtain a wide range of remnant during transformer de-energization. To realize this, controlled “switching off” of the transformer is necessary. A circuit breaker main coil (Fig.8.[a]) along with its auxiliary control circuit (Fig.8.[b]) is included in the main power circuit for this operation. The auxiliary controller actuates the relay (Fig.8.[a]) to trip, which in turn initiates the CB to break contact with the supply main. In the auxiliary circuit switching command (i.e., ON/OFF) is given to the D-FF by a bounce-free switch. The clock pulse to the FF is phase shifted with respect to main supply by an adjustable R, C phase shifter. After receiving the OFF data, D-FF triggers the relay to de-energize the main coil of CB and contact was broken. In this way, arbitrary current chopping operation is carried out at different supply voltage point resulting in a different level of residual flux levels. Typical waveforms shown in Fig.4 indicates how the magnetizing current was chopped other than the natural zero-crossing point.

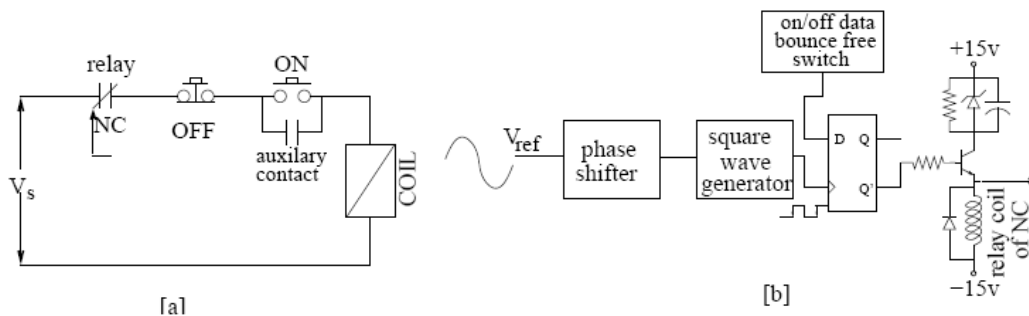


Fig.8. Circuit breaker main coil along with relay and auxiliary control circuitry used to de-energize transformer.

IV. EXPERIMENTAL RESULTS

The controller was tested on a laboratory transformer to verify its ability to eliminate inrush under arbitrary switching conditions. Current probe and voltage sensors are incorporated in the main power circuit to track the instantaneous value of the core flux, magnetizing current, status of the transformer etc. This scheme tracks and records the manner in which core flux settles to different residual level during abrupt de-energization (as shown in Fig.2). After each successive interruption, the controller eliminates the magnetizing inrush current whenever

the supply is re-established. The brief survey of the proposed inrush mitigation techniques along with some typical experimental results are presented below in Fig.9, Fig.10, Fig.11 and detailed explanations are also given below.

TABLE I

TRANSFORMER RATING SPECIFICATION

Parameter	Value
Rating	5 kVA
Primary voltage	230 V(RMS)
Secondary voltage	230 V(RMS)
Frequency	50 Hz
Leakage inductance	9.29 mH
Winding resistance	0.825 Ω
Core resistance	0.35 K Ω

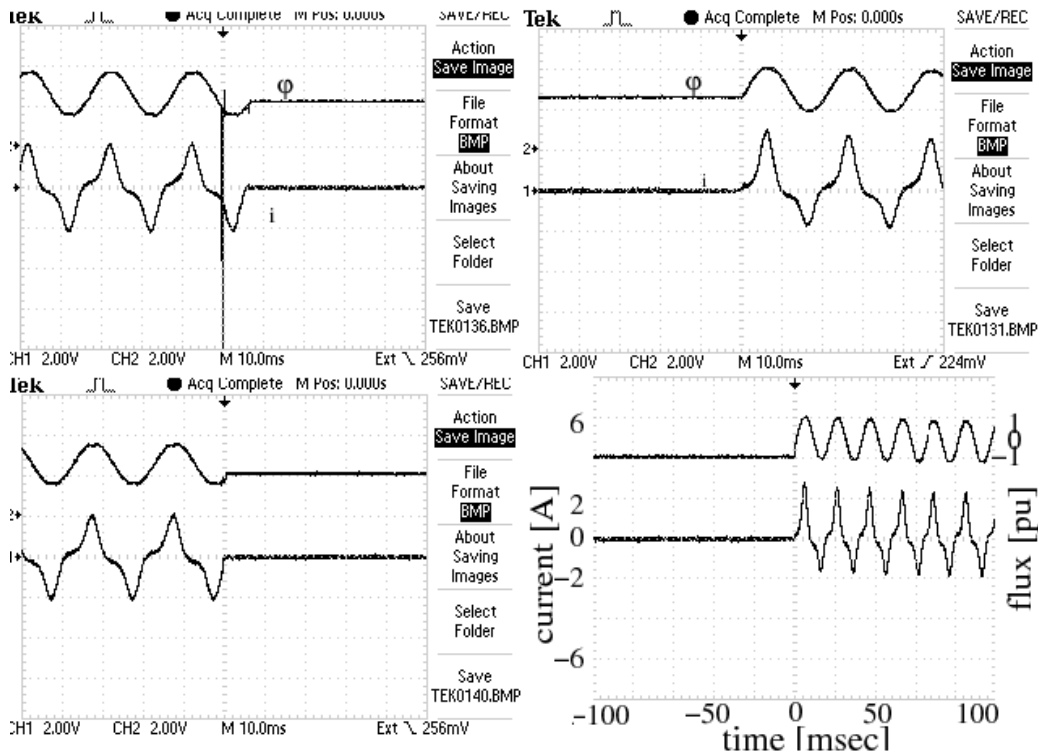


Fig.9. Test results of current and flux waveforms for arbitrary de-energization and next controlled energization instants; resulting residual flux levels ϕ_r settles to a value -0.37 pu (top) and $\phi_r = -0.417$ pu (bottom). Here CH1 of CRO records current 1V=1A, CH2 of CRO records flux magnitude, 1V = 1T.

A. No-Load Test

First the scheme was tested on a single-phase transformer (rating given in Table.1), under no-load. The CB was opened to carry out first arbitrary current chopping operation, by giving an OFF command to the auxiliary control circuit of CB. Now the controller accordingly tracks the core flux transients to store the last value of remnant. Then the CB is again made-ON to re-energize the transformer. After 3-4 cycles delay, the controller sends the firing pulse to triac for actual re-energization. The time delay is provided to avoid the CB pre-strike effect and to allow the dc offset of prospective flux to die down. After each successive interruption, the scheme on-line eliminates the magnetizing inrush current, whenever the supply is re-established. Only initiating ON and OFF command are given to the logic circuit by a push button switch. When the same operation (i.e., arbitrary de-energization and successive re-energization) was carried out without controller switching-ON inrush current was found to be very high (shown in Fig.16 [c]).

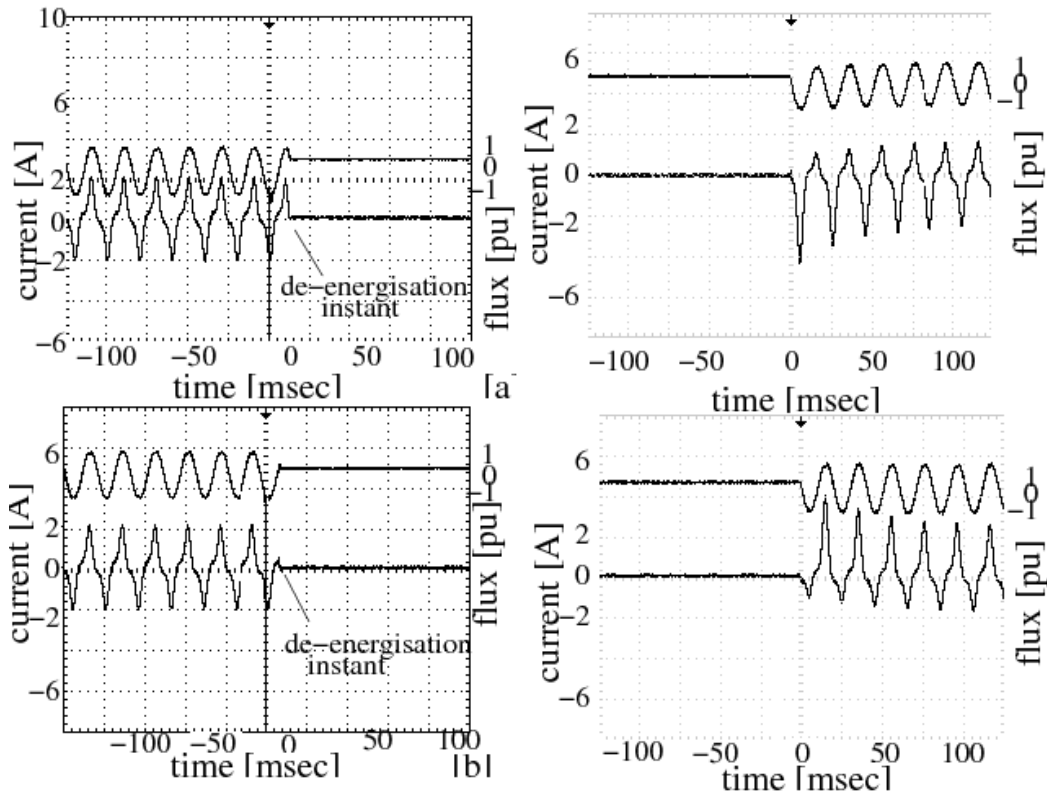


Fig.10. Arbitrary de-energization resulting in +ve residual flux level (current and voltage waveform) and next controlled energization of transformer is done by the controller, resulting flux and current transients: (a) $\phi_r = 0.44$ pu, (b) $\phi_r = 0.378$ pu (Experimental results).

In experimental details, switching instants are expressed in terms of switching angle α . The magnetizing current peak was found to be 2.1 Amp during steady-state operation. Representative results are noted in Table.II and in Fig.12. The following conclusions may be inferred from the results.

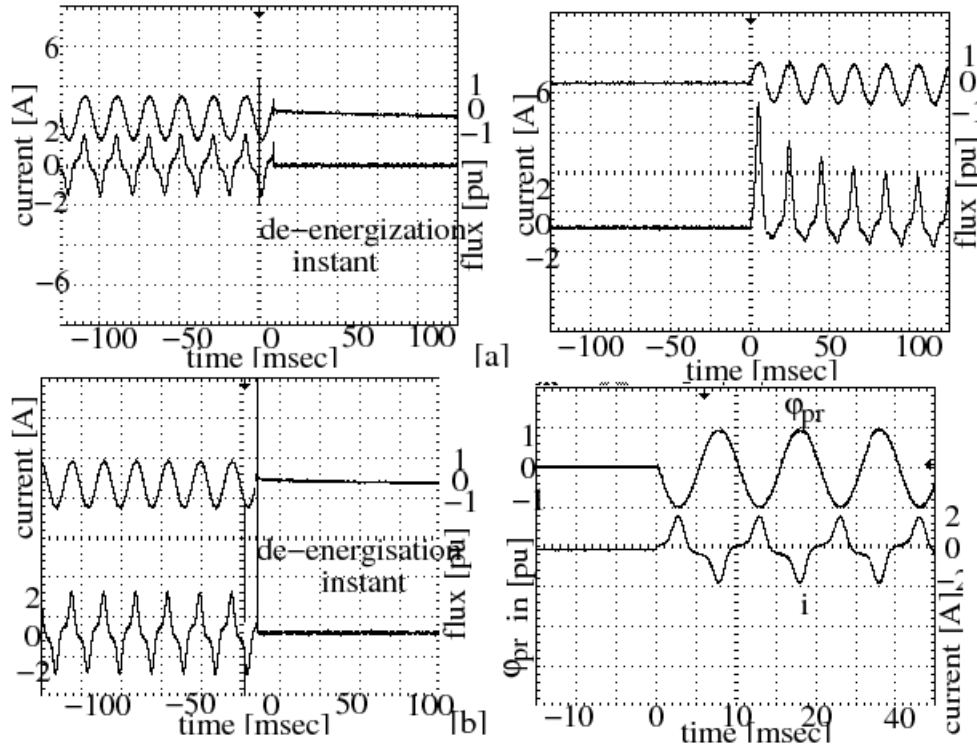
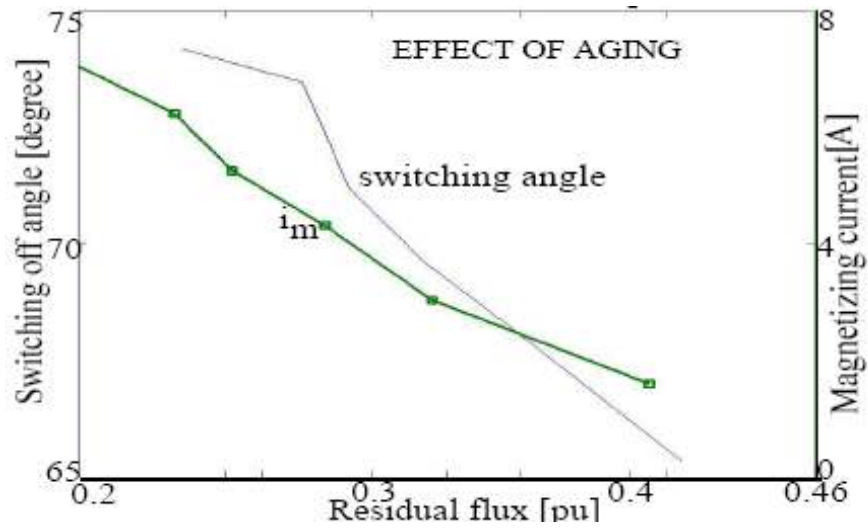
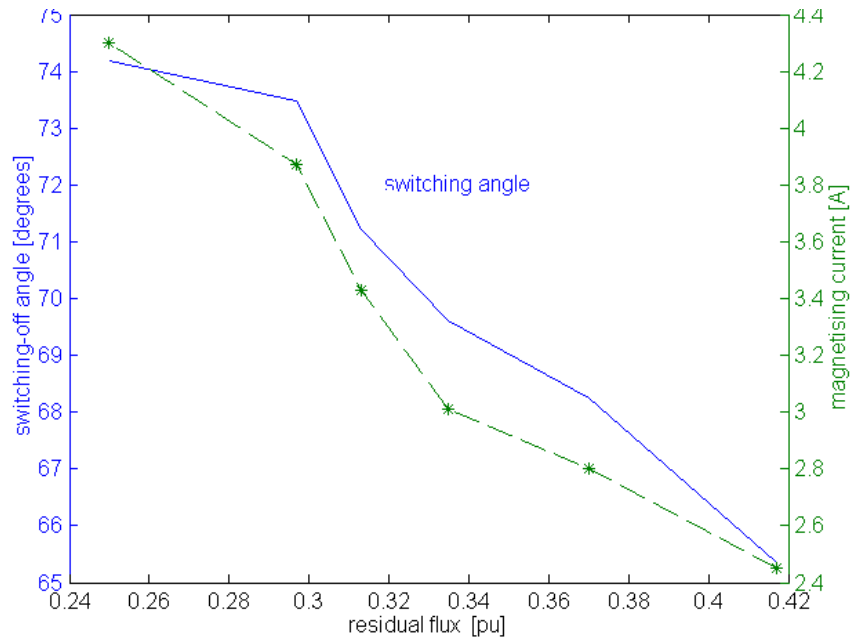


Fig.11. Different cases of de-energization and next, re-energization transients: (a) $\phi_r = 0.17$ pu, (b) $\phi_r = 0$ pu using proposed controller (Experimental results).

TABLE II

VARIATION OF RESIDUAL FLUX AND SWITCHING-ON TRANSIENT CURRENT FOR ARBITRARY SWITCHING OPERATIONS

Actuating turn-off instant α	Actual turn-off instant α	CB Opening time	Chopping Instant current	ϕ_r at turn-off instant	Φ_{cr} at switch-on instant	i_m peak at energization	α at switch-on instant
-128°	68.287°	6.9 ms	-0.8 A	-0.37 pu	-0.371 pu	2.8 A	68.5°
45.85°	65.357°	1.08 ms	-0.21 A	-0.417 pu	-0.417 pu	2.45 A	65.41°
-167°	-64°	14.2 ms	-2.2 A	0.44 pu	0.44 pu	-3.6 A	-64.07°
-141°	112.207°	8.3 ms	-2.04 A	0.378 pu	0.378 pu	3.9 A	67.8°
-131°	99.786°	7.88 ms	1.87 A	0.17 pu	0.17 pu	5.2 A	80.22°
-144°	103°	8 ms	1.76 A	-0.01 pu	-0.01 pu	2.3 A	90°



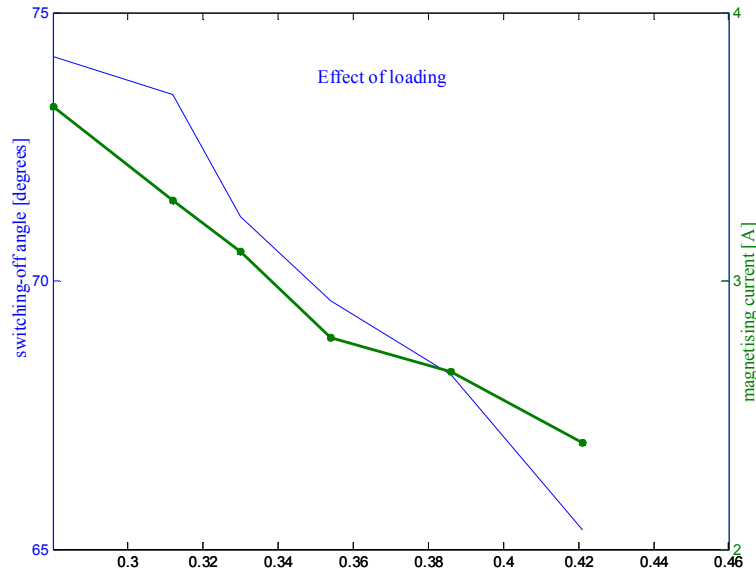


Fig.12. Variation of residual flux levels and magnetizing current i_m peak for arbitrary de-energization and variation of subsequent optimal switch-on instances for different arbitrary de-energization. These variations are also plotted under effect of loading and Effect of aging.

- Current can be chopped in both positive and negative half cycles resulting in +ve and -ve value of remnant.
- Switching under this scheme limits the maximum value of flux growth to utmost 1.1 times of its steady-state value.
- When the remnant value differs large as compared to the steady-state remnant, then switching transients will be more due to large value of current error.
- Subsequent energization and de-energization instants (voltage, flux and current patterns) are nearly identical.

B. Effect of Loading

The performance of the controller was also tested on the same transformer with load to confirm its independent operation. The sampled results are shown in Fig.13 and the findings are noted in Table. III. The following points summarize the effect of loading:

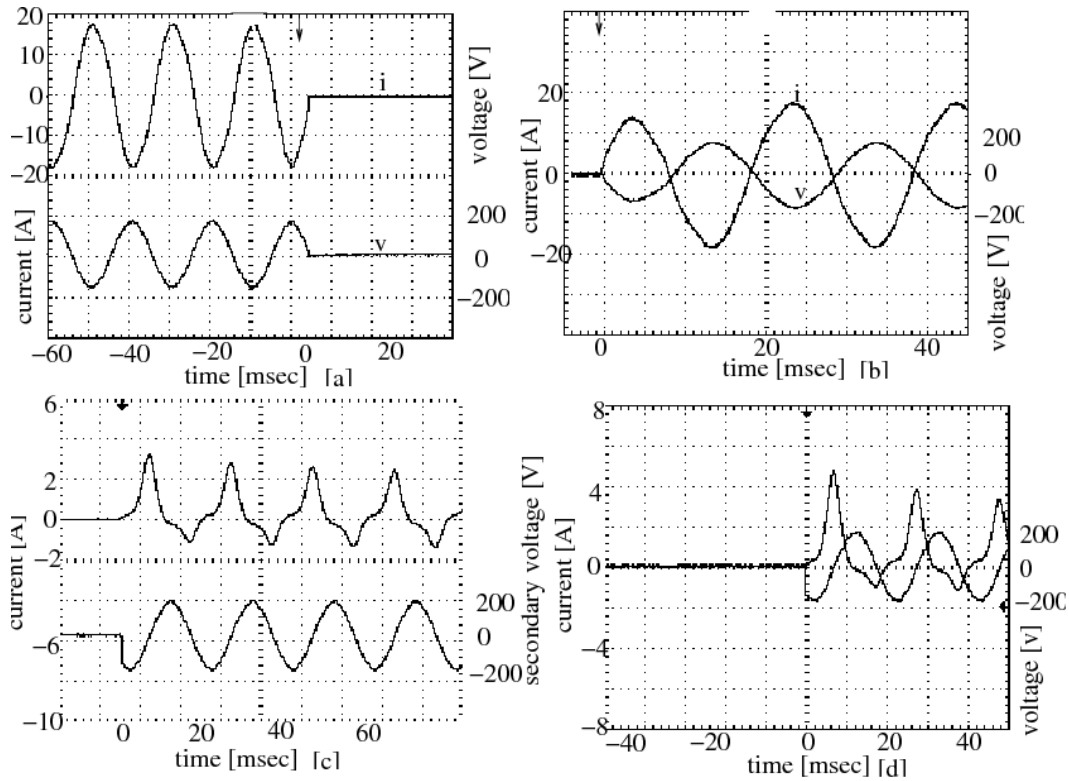


Fig.13. Effect of loading during [a] de-energization, [b] next ON-load re-energization, [c] and [d] next re-energization at no-load (experimental results).

- Switching off voltage and flux transients are less compared to no-load de-energization. This may be due to the increased value of damping constant with secondary loaded.
- Remnant settles to a higher value as compared to steady state remnant. e.g. Consider the 1st case of de-energization of Table. II, earlier remnant has settled to 0.37 pu, but after loading the remnant level is increased to 0.385 pu. This results into 2.33 A of peak current inflow during next re-energization.
- On-Load re-energization reduces the switching transients still lesser. This is because the transient load current decays faster without driving core into saturation.

TABLE III

SWITCHING CURRENT TRANSIENTS (PEAK) UNDER VARIOUS SWITCHING CONDITIONS:
EXPERIMENTAL AND SIMULATED RESULTS

Methods	At $B_r = +ve$	At $B_r = 0$	At $B_r = -ve$	Aging effect	With load
Experimental	2.8-5.9 A	2.2-4.4 A	2.3-4.6 A	2.8-5.8 A	2.51-5.3 A
Numerical	2.6-5.64 A	2.24-4.23 A	2.37-4.5 A	2.67-5.7 A	2.45-5.15 A

C. Effect of Aging

The effect of aging on the controller performance was studied in the following manner. Initially transformer was de-energized by the controller. After two weeks when it was re-energized, switching transients are found to be more prominent compared to the normal operating switching-ON transients. As ferromagnetic core undergoes some aging effect, the actual remnant has reduced a bit from the last stored remnant value, which resulted in more switching transients. For same switching-off instant, $\alpha=128^\circ$ remnant level settles to 0.357 pu instead of 0.37 pu (as shown in Fig.4). This results into a current peak of 4.33 Amp during next re-energization. The effect of aging is shown in Fig.14 and Table. III.

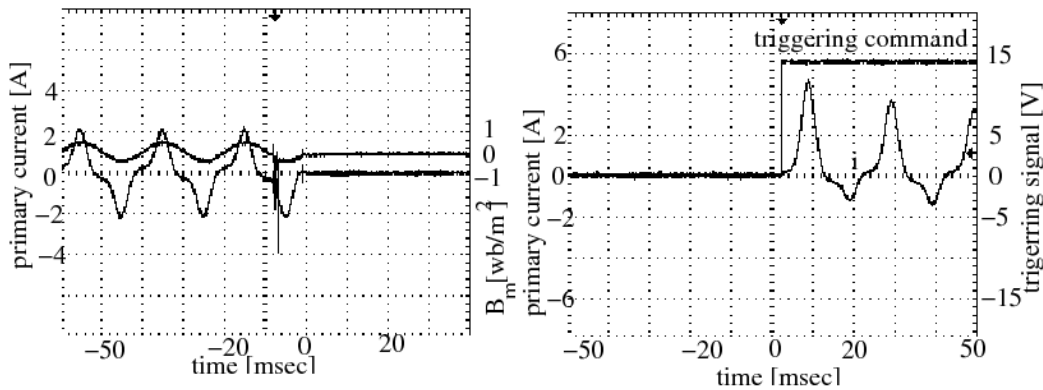


Fig.14. Typical switching-OFF transients and switching-ON transients when re-energized after 2 weeks in closed loop (Experimental results).

V. TRANSFORMER MODELING

Under electric utility power system analysis, it is sometimes necessary to know the dynamic behavior of transformer. The solution of any electric circuit is only accurate if the circuit elements are validly modeled. So, in this theoretical approach transformer is modeled in terms of some linear and non-linear circuit parameters. The non-linearity of the ferro-magnetic core is defined and estimated

by a function called Jile's function. Then its operating performance at any arbitrary instant is determined with the help of those parameters and the input excitation conditions. The model was tested to simulate any abrupt de-energization and re-energization process and the resulting transformer behavior. By implementing the same control switching logic (as used in practical circuit), transient phenomenon of the transformer under controlled switching are simulated and the results are presented.

A. Circuit Modeling and Simulation

The transformer equivalent electrical representation is derived from both physical and magnetic models by principle of duality. As per the flux distribution, the magnetic circuit is represented by mmf sources, non-linear reluctance of the core and linear reluctance of leakage air path (as per Yacamini and Bronzeado(1994), Bronzeado and Yacamini(1995)). The above representation is translated in terms of an equivalent electrical circuit and is represented by some lumped linear and non-linear inductances, resistance and capacitance as shown in Fig.15. In this circuit representation, the non-linear inductance of the core mainly decides the amount of magnetizing current as well as circuit behavior at different operating condition (during switching transient operation, steady state and saturation zone operation). This inductance also determines the remnant left in the core after de-energization. The emf equation of the transformer is:

$$V_s = r_p i_p + N_p \frac{d\phi_p}{dt} \quad (1)$$

The total flux ϕ_p linked with the primary winding can be distributed as leakage flux (through different air paths and inter winding spaces) and the main working flux through the core. As the leakage path offers linear reluctance, they are represented by linear inductances. Whereas the magnetic core having both non-linearity and hysteresis is represented as non-linear inductance. The inter-turn capacitance c_p , c_s and inter-winding capacitance c_{ps} are not effective at low frequency of operation. The circuit equation during on condition is therefore modified.

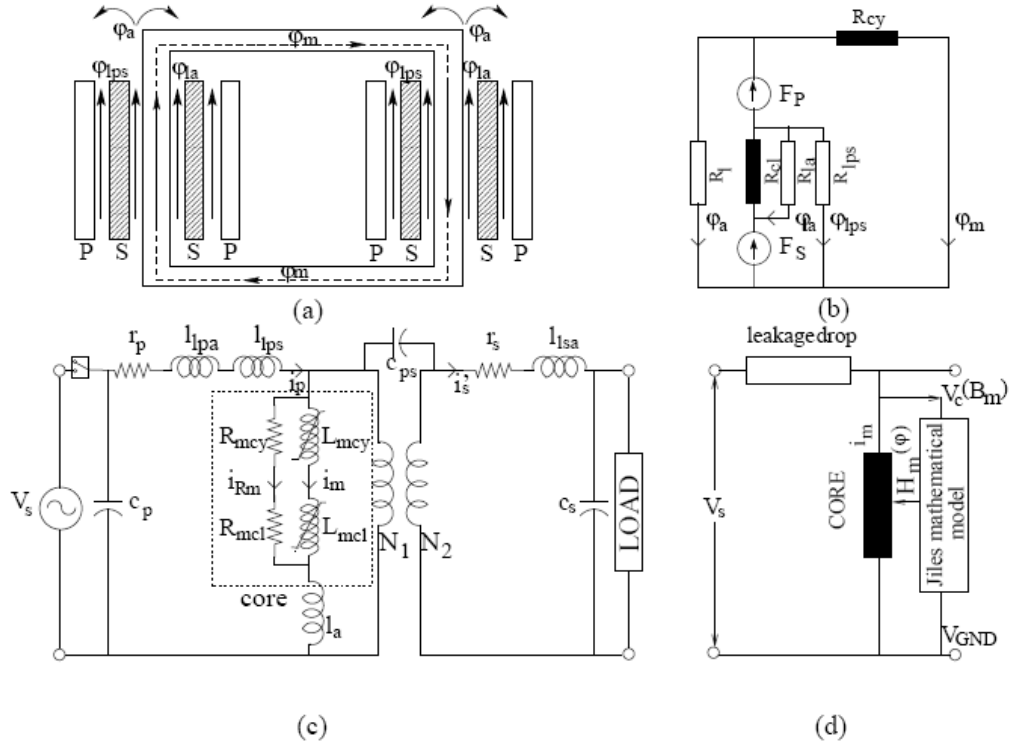


Fig. 15. Single phase core type transformer (a) flux distribution (b) Magnetic equivalent circuit (c) Electrical circuit representation (d) non-linear mathematical model

$$V_s = r_p i_p + l_{lpa} \frac{di_p}{dt} + l_{lps} \frac{di_p}{dt} + l_a \frac{di_m}{dt} + N_p \frac{d\phi_m}{dt} \quad (2)$$

$$V_s = r_p i_p + l_{lpa} \frac{di_p}{dt} + l_{lps} \frac{di_p}{dt} + l_a \frac{di_m}{dt} + N_p A_p \frac{dB_m}{dt} \quad (3)$$

Then, the incremental flux density of the core is given by

$$\frac{dB_m}{dt} = \frac{1}{N_p A_p} \left[V_s - r_p i_p - l_{lpa} \frac{di_p}{dt} - l_{lps} \frac{di_p}{dt} - l_a \frac{di_m}{dt} \right] \quad (4)$$

Usually l_a is neglected in absence of zero sequence current path in single-phase transformer. The primary current is:

$$i_p = i_m + i'_s + i_{Rm} \quad (5)$$

Where:

i_m : magnetizing current

i_s : reflected current

i_{Rm} : loss component of current

i_p : primary current

and at no-load, $i_s = 0$

Again for ferromagnetic core,

$$B_m = \mu_0 (H + M) \quad (6)$$

For exact prediction of core behavior, magnetization within the core is defined as a function of magnetic field intensity as suggested by Jiles and Atherton(1984).

$$M = \mathfrak{F}(H) \quad (7)$$

Where, \mathfrak{F} is Jile's function, and it is dependent on certain parameters (like K , α , M_s .. etc). These parameters for the test transformer is determined from its steady state magnetization characteristics and anhysteretic magnetization characteristics in a similar manner as reported in Jiles et al.(1992). The number of turns, maximum flux linkage of the test transformer was obtained by placing one search coil in the close vicinity of the core. Now, using those parameter and earlier H and B_m values, \mathfrak{F} is evaluated in each step and the corresponding M is updated. Then,

$$\frac{dB_m}{dt} = \mu_0 \left(1 + \frac{dM}{dH} \right) \frac{dH}{dt} \quad (8)$$

equating (4) and (8):

$$\mu_0 \left(1 + \frac{dM}{dH} \right) \frac{dH}{dt} = \frac{1}{N_p A_p} \left[V_s - r_p i_p - l_{lpa} \frac{di_p}{dt} - l_{lps} \frac{di_p}{dt} - l_a \frac{di_m}{dt} \right] \quad (9)$$

Thus by incrementing the calculated dH (from equation 9), H is updated and corresponding magnetization current and primary current are calculated using:

$$i_m = \frac{HL}{N_p} \quad (10)$$

$$i_{Rm} = \frac{N_p}{R_m} \frac{d\phi_m}{dt} \quad (11)$$

Solving simultaneous equation (7), (8), (9) and (10) current, instant to instant B , H values can be estimated. The resulting magnetization curve can also be simulated for any arbitrary instant switching-ON operation. The non-linear, multivalued function \mathfrak{S} plays an important role in transformer modeling. For test transformer different parameters of mathematical models are specified in Table. IV. During de-energization process, the mathematical modeling of the transformer is somewhat different. The switching-off instant stored energy is distributed in the resistive part (of CB, core and winding) as heat loss and rest of the energy is retained in form of residual magnetism in the core. Stray capacitances of the transformer as well as source capacitance become effective during switching-OFF. This equivalent capacitance is estimated from current and voltage waveform during arbitrary current chopping operation. Now the circuit equations are modified in the following manner:

$$\frac{1}{C_p} \int i_p dt + l_p \frac{di_p}{dt} + r_p i_p + e_p = 0 \quad (12)$$

$$e_p = -N_p \frac{d\phi_m}{dt} \quad (13)$$

Then incremental flux density from the modified circuit equation is as follows:

$$\frac{dB_m}{dt} = \frac{1}{N_p A_p} \left[\frac{1}{C_p} \int i_p dt + l_p \frac{di_p}{dt} + r_p i_p - N_p \frac{d\phi_m}{dt} \right] \quad (14)$$

l_p, r_p : represents the equivalent leakage inductance of primary and effective resistance of the winding.

C_p : effective capacitance of the equivalent circuit during switching off condition.

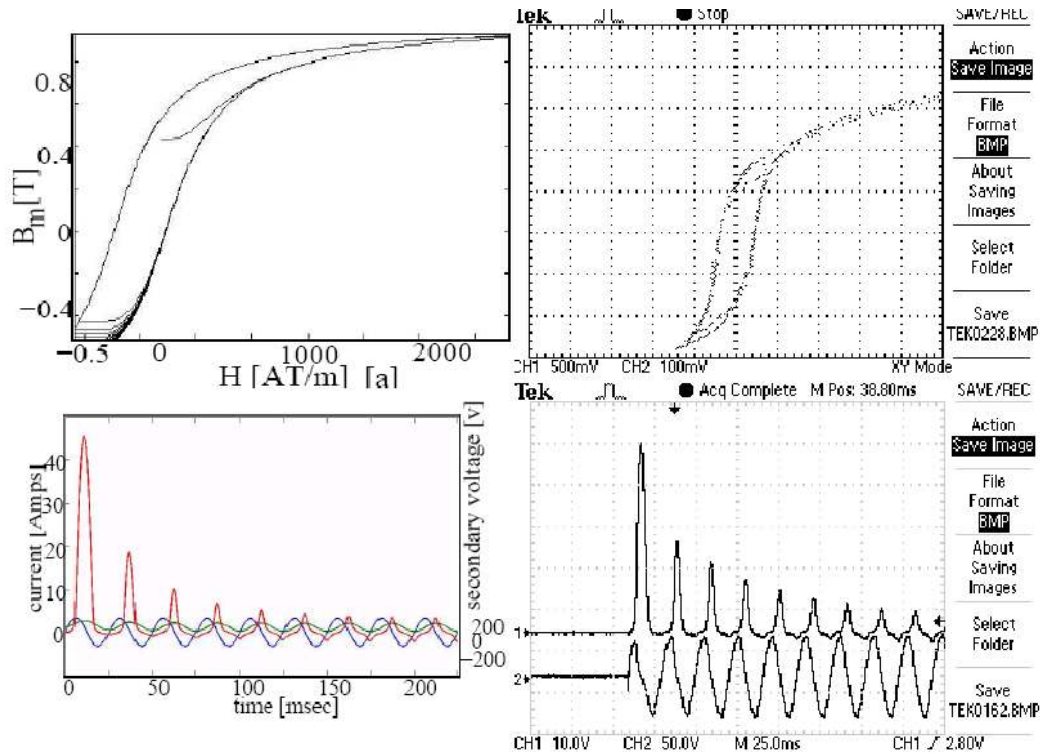


Fig.16. Simulated and experimentally obtained waveform of transformer Dynamic B-H loop and the results of corresponding switching transients : both Simulated (a), (c) Experimental 100 mV = 0.4 T, 500mV = 1KAT/m (b), (d) 1V = 10A, 1V = 100V.

TABLE IV

MODEL PARAMETER

	Hysteresis	Circuit	Physical
K	31.072 $\mu\text{H/m}$	V_s 220V	L 2m
M_s	0.8 MA/m	f 50Hz	A_c 0.000694 m^2
μ_0	0.1257 $\mu\text{H/m}$	B_m 0.8T	N_s 188
c	0.0075	R_m 0.35 K Ω	N_p 188
α	0.000641	r_p 0.825 Ω	
T_s	1 μs	l_p 9.29 mH	
a	342.36 A/m	S 5 kVA	

Due to ferromagnetic and hysteresis behavior, flux within the core builds up in a similar manner as described earlier in equation (7). So,

$$\frac{dB_m}{dt} = \mu_0 (1 + \mathfrak{I}'(H)) \frac{dH}{dt} \quad (15)$$

Both $\mathfrak{I}(H)$ and $\mathfrak{I}'(H)$ can be calculated in the same way as described during on condition. Then equating the above two equations, incremental magnetic field intensity within the core is calculated as follows:

$$\mu_0 \left(1 + \frac{dM}{dH} \right) \frac{dH}{dt} = \frac{1}{N_p A_p} \left[\frac{1}{C_p} \int i_p dt + l_p \frac{di_p}{dt} + r_p i_p - N_p \frac{d\phi_m}{dt} \right] \quad (16)$$

Solving simultaneous equation (15), (16), (10) and (11), instantaneous B_m , H , dM/dH and i_m value is estimated and updated. After very small time span, incremental flux density becomes zero. That instant intrinsic magnetic field intensity or magnetization corresponds to the “remnant” of the core for the specific switching-OFF condition. In this manner, switching-OFF transient behavior of the test transformer is simulated and resulting remnant value is estimated.

B. Simulation Results

Simulation studies have been carried out to show the time dependent relationship among current voltage and flux, the operating performance under various operating conditions. Several sets of experiments and simulation are carried out by controlling the switch-ON point and the residual flux level by energizing and de-energizing at different instants of supply voltage waveform. The results obtained are noted and compared in Table. III and Table. V. Experimental and simulation results for two different cases one with inrush and one in steady states are shown respectively in figures (Fig.15) and in (Fig.16). Another two instants (one with initial +ve remnant and other with -ve remnant) of inrush free switching transients are shown in Fig. 18 and their initial dynamic magnetization characteristics are presented. Those results adequately describe validity of the theoretical model with controlled switching scheme.

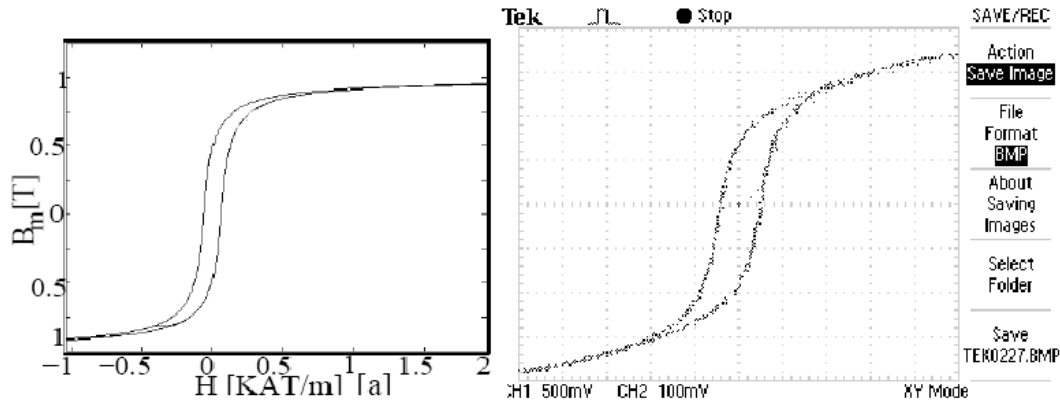


Fig.17. Comparison of steady state hysteresis curve obtained from simulated [a] and experimental studies[b]; Here CH1 records H value and $1V=0.5$ KAT/m, CH2 records B_m value; 200 mV= 0.4 T.

TABLE V

COMPARISON OF B-H CHARACTERISTICS AT DYNAMIC AND STEADY STATE : EXPERIMENTAL AND SIMULATED RESULTS

Experimental		Numerical	
Steady state maximum B_m	0.74 T	Steady state maximum B_m	0.749 T
Steady state maximum i_m	2.43 A	Steady state maximum i_m	2 A
At inrush maximum B_m	1.06 T	At inrush maximum B_m	1.08 T
At inrush maximum i_m	48 A	At inrush maximum i_m	55 A
Steady state remnant B_r	0.46 T	Steady state remnant B_r	0.464 T
Transient remnant B_r	0.6 T	Transient remnant B_r	0.65 T

VI. CONCLUSION

By adopting the controller and implementing proposed control logic, transformer switching inrush is substantially checked. The peak of the inrush current is reduced to almost 1.2 times the normal steady state magnetizing current value. The scheme do not involve any complex numerical analysis, information regarding material characteristics and additional complex circuitry. The working of the controller is independent of the supply impedance and fluctuation. With the above mentioned advantages along with almost transient free operation proves the scheme to be quite effective. The theoretical concept of the proposed approach is supported by appropriate experimental results. The proposed scheme is cost effective, efficient and eliminates inrush in a rather simple manner.

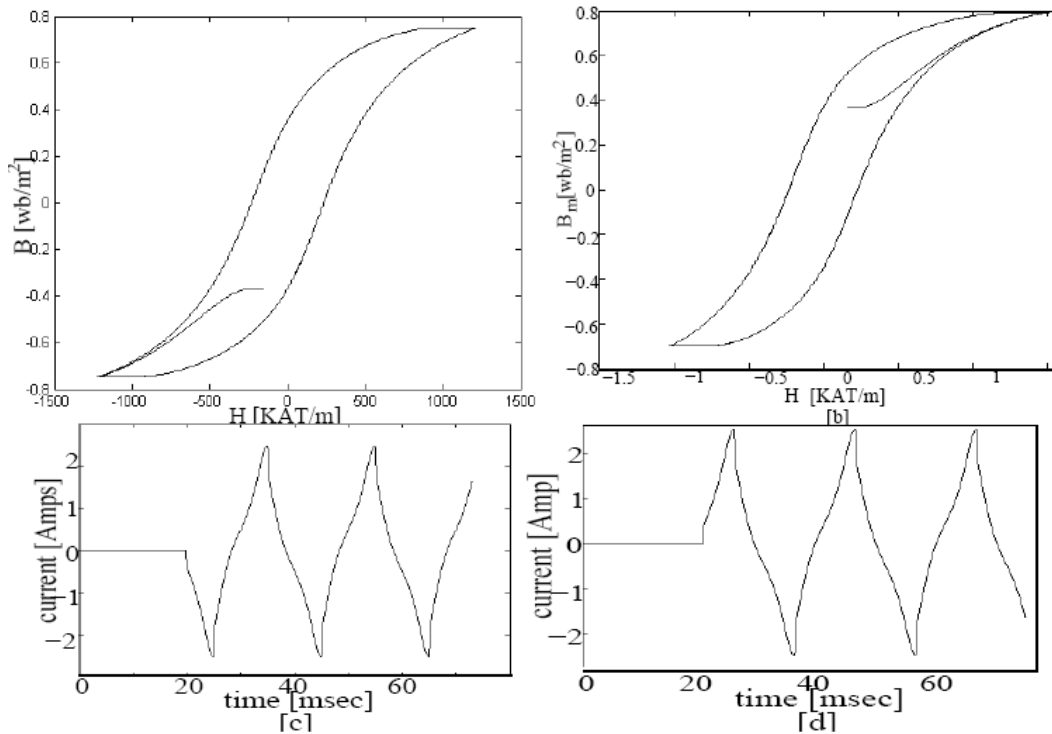


Fig.18. Initial dynamic B-H loop and corresponding switching-ON current waveforms, here controlled switching logic is implemented during energization, (a),(c) energization with +ve B, and (b), (d) energization with -ve B, (Simulated results).

REFERENCES

Abdulsalam, S.G. and Xu, W.(Jan 2007).: A sequential phase energization technique for transformer inrush current reduction Part-II: Transient performance and practical considerations, IEEE Transactions on Power Delivery, vol.22, no.1, pages.208-216.

Al-Khalifah, A.K. and El-Saadany (2006).: Investigation of magnetizing inrush current in a single phase transformer, Large Engineering System Conference 2006, Power Engineering, pages.165-171.

Asghar, S.J.(Jan 1996).:Elimination of inrush current of transformers and distribution lines, Proceedings of International Conference on Drives and Energy Systems for Industrial growth, Power electronics, vol.2, pages.976-980.

Bronzeado, H. and Yacamini, R.(July 1995),: Phenomenon of sympathetic interaction between transformers caused by inrush transients, *Sci.Meas.Technol., IEE Proceedings*, vol.142, no.4, pages.323-329.

Brunke, J.H. and Frohlick, K.J.(April 2001a),: Elimination of Transformer inrush current by controlled switching, Part-I: Theoretical considerations, *IEEE Transactions on Power Delivery*, vol.16, pages.276-280.

Brunke, J.H. and Frohlick, K.J.(April 2001b),: Elimination of Transformer inrush current by controlled switching, Part-II: Application and Performance considerations, *IEEE Transactions on Power Delivery*, vol.16, no.2, pages.281-285.

Cheng, C.K., Liang, T.J., Chen, J.F., Chen, S.D. and Yang, W.H.(May 2004),:Novel Approach to reducing inrush current of power transformer, *Electric Power Applications-IEE Proceedings*, vol.151, no.3, pages.289-295.

Cui,Y., Abdulsalam, S.G.,Chen, S. and Xu, W.(April 2005), : A sequential phase energization technique for transformer inrush current reduction Part-I: Simulation and Experimental results, *IEEE Transactions on Power Delivery*, vol.20, no.2, pages.950-957.

Jiles, D.C. and Atherton, D.L.(March 1984),: Theory of Ferromagnetic hysteresis, *Journal of Applied Physics*, vol.55, no.6.

Jiles, D.C., Thoeke, J.B. and Devine, M.K.(Jan 1992),: Numerical determination of hysteresis parameters for the modeling of magnetic properties using theory of ferromagnetic hysteresis, *IEEE Transactions on Magnetics*, vol.28, no.1.

Kaszteny, B.(April 2006),: Impact of transformer inrush currents on sensitive protective functions, how to configure adjacent relays to avoid nuisance tripping, *59 th Annual Conference for Protective Relay Engineers, 2006*, page.21

Len, C.E., Cheng, C.L., Huang, C.L. and Yeh, J.C.(Jan 1993),: Investigation of magnetizing inrush current in transformer. I.Numerical simulation, *IEEE Transactions on Power Delivery*, vol.8, no.1, pages.246-254.

Ling, P.C.Y. and Basak, A.(Nov 1988),: Investigation of magnetizing inrush current in a single phase transformer, *IEEE Transactions on Magnetics*, vol.24, no.6, pages.3217-3222.

Ogawa, M.(May 2002),: Magnetizing inrush current of a transformer and a new technique of its computation, ISCAS 2002, IEEE International Symposium on Circuits and Systems 2002, vol.3, no.6, pages.417-420.

Shyu, J.L.(Nov 2005),: A Novel control strategy to reduce transformer inrush current by series compensator, Power Electronics Drives and Systems, International Conference on PEDS 2005, vol.2, pages.1283-1288.

Steurer, M. and Frohlich, K.J.(Jan 2002),: The impact of inrush currents on the mechanical stress of high voltage power transformer coils, IEEE Transactions on Power Delivery, vol.17, no.1, pages.155-160.

Xu, W., Abdulsalam, S.G., Cui,Y. and Liu, X.(April 2005),: A sequential phase energization technique for transformer inrush current reduction Part-II: Theoretical analysis and design guide, IEEE Transactions on Power Delivery, vol.20, no.2, pages.943-949.

Yacamini, R. and Bronzeado, H.(Nov 1994), : Phenomenon of sympathetic interaction between transformers caused by inrush transients ,Sci.Meas.Technol., IEE Proceedings, vol.141, no.6, pages.491-498.